

FINITE ELEMENT ANALYSIS OF RESIDUAL WELDING STRESSES AND DEFORMATION FOR A 5A06 ALUMINUM ALLOY PLATE

N. C. Lü,^{a,1} M. H. Wang,^a G. D. Hao,^{b,2}
and Y. T. Wang^c

UDC 539.4

The residual stresses and deformation, in terms of the thermoelastoplastic theory, were simulated with the finite element method using ANSYS 13.0 software for a 5A06 aluminum alloy plate after welding. The butt joint thickness of the plate was 6 mm. A 3D thermomechanical model of the plate was constructed. The dimensions and distribution of residual stresses in the welded structure should be analyzed after simulation. Appropriate welding technologies were chosen to control welding residual stresses and deformation. The efficient production of an aluminum alloy for the welded structures will be provided.

Keywords: 5A06 aluminum alloy, finite element analysis, ANSYS, residual stress, residual deformation.

Introduction. Aluminum alloy structures have been widely used in transportation, railway, ships, aerospace, aeronautics and other engineering fields, which is one of the aspects of computer applied engineering (CAE). Because of the low elastic modulus of aluminum alloy, its thermal conductivity, linear expansion coefficient and specific heat capacity are higher than those of other metals, such as low-carbon steels, alloy steels, etc., the residual stress and large deformation in the course of welding were inevitably produced after welding structure which would also affect the welding quality and reliability of structures [1]. At the same time, for the aerospace material of aluminum alloy structure, welding residual stress state is very complex. Therefore, it has a lot of important academic values and practical significance to carry out the numerical simulation research on the temperature field and the thermal stress field in the welding process.

In this paper, the butt joint of the 5A06 aluminum alloy plate with a thickness of 6 mm has been simulated as an example. By using the large-scale general tool of finite element analysis software ANSYS 13.0 in [1, 2], the numerical simulation of welding stress field is made on the butt joint of an aluminum alloy plate with a thickness of 6 mm; therefore the evolution and distribution of dynamic welding stress field in the process of welding were studied for further research in this paper. The stress field in the welding process is analyzed, and the residual stress and deformation are observed, which provide scientific references for the actual welding researches.

The 5A06 aluminum alloy, selected as welding material, belongs to the aluminum-magnesium system of anti-rust aluminum, which has high strength and corrosion stability. Under annealing and extrusion conditions, its plasticity is good, while the weld compactness and plasticity can be ensured by using argon arc welding [3, 4], while the strength of the welding joint using gas welding and spot welding is 90–95% of the base metal's one, and the joint has good cutting performance. To improve work efficiency, ensure the welding quality, the welding technology of TIG automatic welding (AC) was adopted, and then the welding simulation was carried on in this paper.

^aSchool of Material Engineering, Shenyang Ligong University, Shenyang, China (¹lnc_65@163.com).
^bDepartment of Chemistry, Mudanjiang Normal College, Mudanjiang, China (²haogudong163@163.com). ^cCollege of Mechanical Engineering, Liaoning Technical University, Fuxin, China. Translated from Problemy Prochnosti, No. 4, pp. 42 – 49, July – August, 2020. Original article submitted May 12, 2020.

The obtained results were more precise than those in [1, 3]. Noteworthy is that software design and technological parameters of aluminum alloys welded by the MIG in [1, 3] were different from those used in this work, because the welding quantity of automatic TIG outperforms that of MIG for the same conditions, while MIG is usually used for welding thin plates, i.e., less than 6 mm.

1. Establishment of Finite Element Model.

1.1. Welding Joints Form and Process Parameters. Considering the practical production of aluminum alloy sheet size, the simulation model dimensions were $250 \times 250 \times 6$ mm. Since the arc moved along a straight line in the middle of the aluminum alloy plate, only a half of the model was meshed and simulated. Using automatic TIG welding, the butt joint was formed in this paper. The argon arc welding machine type [5] was AEP-500, rated output voltage of 380 V, the rated output current of 500 A, the rated input current was 113 A, and the rated load voltage was 40 V. According to [5], the welding parameters used in the simulation were: arc voltage of 25 V, welding current of 300 A, welding speed of 5 mm/s, welding thermal efficiency of $\eta = 0.8$, and effective heating arc radius of 8 mm.

1.2. Geometric Modeling and Meshing. To calculate the welding residual thermal stress of the 5A06 aluminum alloy plate, the indirect method should be used in the course of simulation. Meanwhile, the SOLID70 finite elements should be used in thermal calculation. The table-drawing cell method is adopted in the calculation of heat, so one should use the PLANE55 plane thermal unit and SOLID185 to calculate stresses. To ensure the precision of calculation, using of encryption mesh near the weld, the mesh size of 1.2 mm was controlled, while a sparse grid was adopted for the distant zone from the welding. More detail on the model and meshing can be found elsewhere [6].

1.3. The Selection of Heat Source Model. In TIG welding, the Gauss heat source was used for the arc simulation, which was derived as follows.

The heat flux density [6] of point A from any distance of the heating center can be expressed in the following form:

$$q(r) = q_m \exp\left(-\frac{3r^2}{R^2}\right), \quad (1)$$

where $q(r)$ is any point of heat flux of heating spots center, q_m is the maximum heat flux of heating spots' center, R is the effective heating arc radius, and r is the distance between point A and the heating spot center.

For the moving heat source in reference [6] expression is the following form:

$$q_m = \frac{3Q}{\pi R^2}. \quad (2)$$

The heat source model is widely used in the finite element analysis method, in order to calculate the welding temperature field. In the case of small arc and low impact force of the weld pool, the more accurate results can be obtained by means of this model.

1.4. Define Material Properties. The mechanical properties and physical properties of materials are the most important physical unit in the process of numerical simulation of temperature field, which play a decisive role in the accuracy of the simulation results to decide whether the result is correct or not. Parameter parts were adopted in the study cited from the literature data [7]. The high-temperature parameters are obtained by using appropriate extrapolation of the low-temperature parameter curve. In this paper, the simulation parameters of the aluminum alloy are shown in Table 1, according to [7].

Table 1 narrated the relation between thermophysical properties of aluminum alloys and temperature, and it is cited in [8]. Under the action of welding high temperature arc (up to 8,000–10,000°C) of TIG, the temperature of the molten pool in the welding process easily exceeds the melting point of aluminum alloy, which leads to the instantaneous melting and rapid solidification of metal at welding site with the movement of welding arc.

1.5. Simulation of Boundary Conditions. Heat calculation: the initial temperature of the welding is 20°C, meanwhile the upper and lower two surfaces of the welding parts as well as the surrounding three surfaces are heat

TABLE 1. Thermophysical and Mechanical Parameters of the Weld Sample

Temperature (°C)	Thermal conductivity (W/m·°C)	Density (kg/m ³)	Specific heat (J/kg·°C)	Poisson's ratio	Expansion coefficient (m/°C)	Elastic modulus (GPa)	Yield stress (MPa)
20	118	2660	924	0.31	22.8·10 ⁻⁶	68.0	160
100	121	2600	921	0.32	24.7·10 ⁻⁶	62.0	150
200	126	2550	1005	0.31	26.5·10 ⁻⁶	55.5	125
300	130	2500	1047	0.35	27.0·10 ⁻⁶	44.0	80
400	138	2490	1089	0.30	27.8·10 ⁻⁶	48.0	55
600	118	2350	1390	0.32	27.5·10 ⁻⁶	28.0	21
800	116	2300	1200	0.31	26.5·10 ⁻⁶	18.0	18
1200	122	2300	1010	0.31	26.0·10 ⁻⁶	16.0	15
1500	128	2300	1005	0.33	25.8·10 ⁻⁶	15.0	15

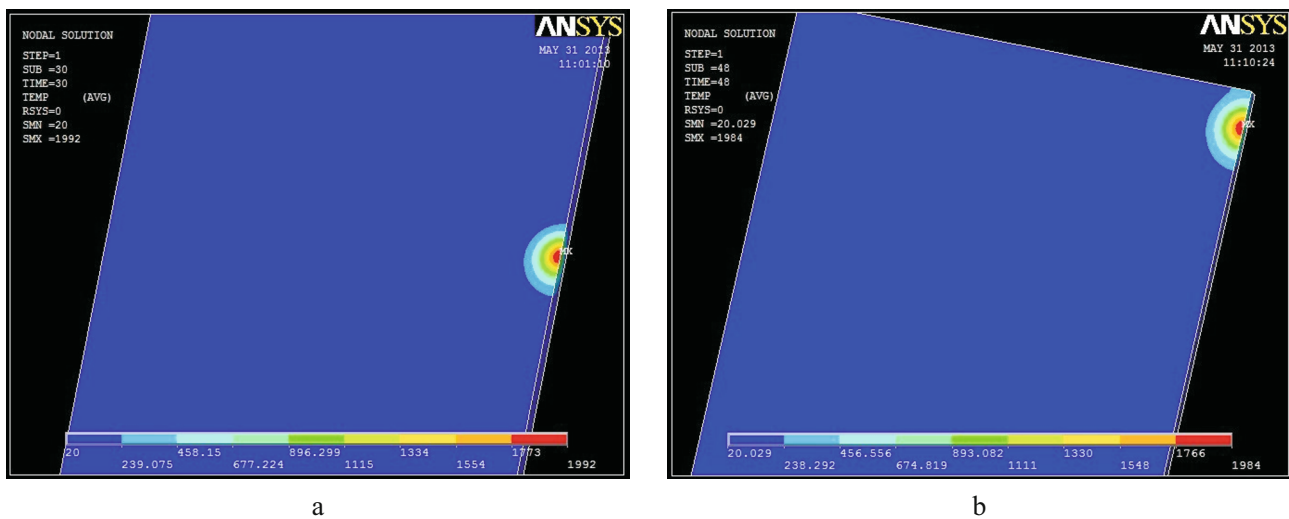


Fig. 1. Welding temperature field at the different time: (a) 10 s; (b) 48 s.

transfer of convection. The convective heat transfer coefficient is 20, and the symmetrical surface of the welding parts are insulated.

Stress calculation: In the finite element analysis, the boundary condition of load-displacement is to prevent rigid displacement during the process of calculation. But the displacement constraint cannot seriously impede the free release and free deformation of the stress during the welding process [8]. The modality of constraint is different because of unlike structure. This test adopted is a flat plate welding, which is used as a bottom surface of a side constraint in the *Y*- and *Z*-directions. The calculation of this example will take about 1000 s, when the plate has been cooled to room temperature, so the stress at this time is the residual welding stress.

2. The Numerical Simulation Results and Analysis.

2.1. Welding Temperature Field. The characteristics of the welding process are that the temperature changes greatly, and the highest temperature can reach the boiling point of the material in the weld zone, while the temperature is sharply decreased to room temperature away from the heat source [9]. The welding process using the Gauss moving heat source for heating, hence the sectional temperature distribution of the welding is a function of time, and the thermal welding stress is due to the uneven heat input. In the correct simulation, the temperature field is the precondition of the residual stress and deformation. When the temperature field of the welding process is shifted from the diagram, the arc movement can be seen in Fig. 1a and 1b, where the temperature field changes after the welding process termination.

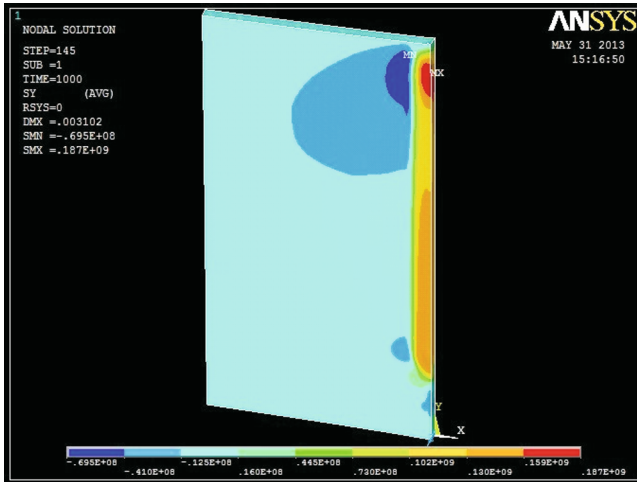


Fig. 2. The longitudinal residual stress distribution.

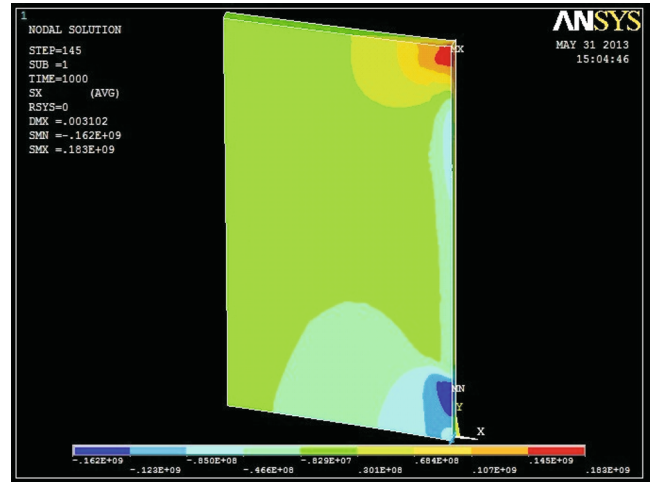


Fig. 3. The transverse residual stress distribution.

As can be seen in Fig. 1b, when the welding time is about 48 s, the moving electric arc heat source generates a moving welding temperature field. On account of the high thermal conductivity of aluminum alloy, the temperature field can be approximated as a standard circle (the heat source center), and the temperature in the middle of the molten pool is 1765°C. Heating spots regarded as the center of the surrounding area will gradually decrease, the welding edge temperature closes to room temperature. In the moving heat source, the first half of the isotherm is dense, while the second half of the isotherm field is sparse. Moreover, it can be seen from the diagram that the temperature of each point changes uniform during the whole welding process, and the temperature of the near weld zone varies rapidly. Away from the weld zone, the temperature changes slowly, and the temperature gradient in the vertical direction of the weld is very large. This kind of high uniform temperature field is the main cause of the residual welding stress. At the beginning of the monitoring point, the room temperature of 20°C that is observed. When the heat source moved closer to the monitoring point for 15 s, the temperature increased rapidly. With the heat source moving away, the temperature drops quickly. The comparison shows that the variable of temperature is the same as the weld centerline. The temperature rise is faster than that of the temperature drop. The temperatures far away weld, which were subjected to the heat source influence was less than those close to the weld. For the point outside the weld centerline, heat conduction is the main reasons during welding, the maximum temperature of each point reduces gradually with the increase of the distance from the center of the weld.

2.2. Stress Field of the Welded Joint. The thickness of the material in the general welding structure is very smaller than its length and width. Mid-thick plate or plate with a thickness below 200 mm are frequently used in welded structures, while welding stresses in the thickness direction are very small, and the residual stress field is in the plane strain state [10]. Only large-scale structures with thick welds has high residual stresses in the thickness direction. In general, the residual stress along the direction of the weld is to be a longitudinal stress, and it is represented by σ_L . The residual stress, which is perpendicular to the direction of the weld, is a transverse stress σ_T . The residual stress in the thickness direction is σ_z . In this study, the thickness of the aluminum alloy plate was 6 mm, so it has two-axial forces. The distribution of the welding residual transverse and longitudinal stresses from the start of welding to cooling to the room temperature are depicted in Figs. 2 and 3, respectively.

2.2.1. The Longitudinal Residual Stress Analysis. The longitudinal residual stress distributional nephogram is given in Fig. 2. It shows the areas where the weld and near-weld zones experience high temperature in butt welding. When the weld is longer, a stable zone will occur in the middle part of the welding seam. The longitudinal residual stress in the stable region will reach the yield strength of the material. At the weld, there exists the stress transition zone, and the longitudinal stress gradually decreases, reaching a zero value at the edge of the plate ($\sigma_L = 0$). In general, when the internal stress direction is normal to the material boundary, the stress at the boundary is zero. If the stress direction and the boundary are not normal, there will be a nonzero shear stress at the boundary.

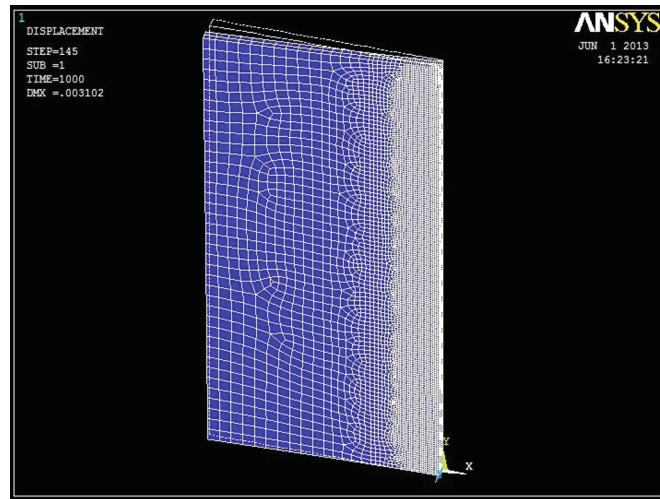


Fig. 4. The model's overall residual deformation.

When the weld length is short, the stress stability zone will disappear, and only transition zone exists. The shorter the weld seam, the smaller the longitudinal stress [10]. From the last figure, the numerical values can be easily extracted, and the obtained pattern is similar to that of study [10].

The distribution of longitudinal stresses along the horizontal section of the plate is a central area which is tensile stress, while the compressive stress distributes along both sides of the weld, tensile stress and compressive stress will balance within section. For aluminum alloy, the distribution of longitudinal stress σ_L is similar to that of low carbon steel. Because of its relatively high thermal conductivity, the aluminum alloy is heated in the process of welding, while its actual limit is smaller than that of the plane assumption. Therefore, the compressive plastic variable will decrease, the residual stress is also reduced, and the general longitudinal residual stress is only $(0.6 \sim 0.8)\sigma_s$.

2.2.2. The Transverse Residual Stress Analysis. The direct cause of the transverse residual stress in Fig. 3 is the horizontal shrinkage of the weld cooling, and the indirect cause is the longitudinal shrinkage of the weld. In addition, different cooling processes at the surfaces and in the bulk, as well as possible superimposed phase transformation, will also influence the distribution of the transverse stress [10]. Therefore, the transverse residual stress σ_T is generally made up of two parts: one part is caused by the longitudinal shrinkage of the weld and the plastic zone near the weld, and the second one is caused by the transverse shrinkage of the weld and its vicinity to the plastic zone near the weld.

Owing to the residual stress caused by longitudinal shrinkage, the stress of the starting and the end of the weld is compressive stress, while the stress in the middle zone is tensile stress. The different time of the transverse shrinkage is caused by the unlike time of heating and the cooling during the course of heat source moving. When heat source is not at the same time, tensile stress formed easily at two ends of the weld while compressive stress formed in the weld middle.

The results are shown in Figs. 2 and 3, the longitudinal residual stress σ_L , the transverse residual stress σ_T , and the maximum value of tensile stress appeared in the weld region. These rules can guide appropriate design welding process in order to reduce residual stress in the practical production.

2.3. Residual Deformation after Welding. Due to the local high temperature heating and rapid cooling in the welding process, thermal strain and compression plastic strain produced in the welding seam and near-weld zone of the parent material, which caused the internal stresses. Eventually the welding deformation will occur. The simulated overall residual deformation can be seen in Fig. 4.

Residual welding-induced deformation is an unavoidable problem in welds. That is, structural deformation occurs after welding, which, in general, will produce the following three basic dimensions of change in the welding:

(1) The transverse shrinkage of the axis perpendicular to the weld line: Transverse shrinkage limited by the base metal is produced in the expansion of the high temperature of the weld metal, and it results in the compression plastic deformation of the whole welding parts in the cooling of the weld.

(2) The longitudinal shrinkage parallel to the weld axis: In the process of welding, the compression zone produced by the welding seam and the near zone are the main causes of the longitudinal deformation.

(3) Angular distortion: As a result of thermal expansion or contraction, it was caused by a change in the angle. The deformation rules of the curved plate of 5A06 aluminum alloy with different thickness is not conclusive. In production, the deformation law of steel is often applied to the aluminum alloy. Because the physical and chemical properties of aluminum alloy are very different from those of the steel, the critical thickness of aluminum alloy cannot be the same, it was impossible to calculate the angular distortion of the welded aluminum alloy using the steel deformation diagram [11, 12]. The welding angular distortion of an aluminum alloy was similar to that of steel, being related to the thickness. When the thickness was less than the plate critical value, i.e., 6–8 mm, the angular distortion was caused by the plate instability. When the plate thickness exceeded a certain value, its angular distortion could only be determined by the transverse shrinkage of the upper and lower surfaces. Hence, the temperature difference determined the angle distortion value. When the thickness of plate was equal to a certain value, i.e., 6–8 mm, its angular distortion was caused by both the temperature difference and instability. Accordingly, this parameter is called the critical thickness and detailed in literature [11, 12]. The critical plate thickness is usually a range, in which there are both temperature difference- and instability-induced angular deformations, so the particular value is hard to determine.

CONCLUSIONS

1. According to thermodynamics principle applied to welding, a 3D transient numerical analysis mode of welding temperature field was constructed for of a 5A06 aluminum alloy plate ($\delta = 6$ mm) butt. The model considered the solid heat conduction of parent metal. With the temperature change of the material, the thermal physical parameters of the welding surface involved the convection and radiation to the surrounding environment, which affected the welding temperature field. The moving Gauss heat source was applied to the workpiece as a thermal load.

2. The temperature field and the thermal cycle curve of feature points in the aluminum alloy plate butt welding were obtained. The calculation results show that the aluminum alloy's thermal conductivity is higher, the linear expansion coefficient is larger, and the temperature field is approximately circular. Because of different heating periods, the model varies greatly along the weld length direction, which makes a great difference between the temperature field and the plane hypothesis. The position of the peak temperature of the thermal cycle curve of each point will change with the different welding sequence. The maximum temperature of each point reduces gradually with the increase of the distance from the center of the weld.

3. Residual deformation of the aluminum alloy plate of butt welding was obtained by simulation calculation. It is can be seen that the higher the aluminum alloy line expansion coefficient and thermal conductivity rate is, the larger aluminum alloy produce deformation will produce, because the temperature field of aluminum alloy is approximately circular which contradicts the plane hypothesis.

4. For the aluminum alloy, the distribution of longitudinal stress is basically similar to that of low carbon steel, the actual restriction of thermal expansion of aluminum alloy in the welding process is smaller than that implied via the plane hypothesis because of its high thermal conductivity, so the compressive plastic deformation and the residual stress decreased, while residual stress could reach only $(0.6 \sim 0.8)\sigma_s$.

Acknowledgment. The research was supported by the National Natural Science Foundation of China (51672120).

REFERENCES

1. Y. X. Zhu, Q. Wang, and X. R. Zhao, "The simulation of welding residual stress based on ANSYS 2004," *J. Wuhan University of Technology*, **02**, 14–21 (2013).

2. D. J. Yan, X. S. Liu, and J. G. Yang, "The influence of thermal physical parameters on the peak characteristics of welding residual stress by finite element analysis," *Trans. China*, **45**, No. 6, 123–132 (2010).
3. Z. M. Fu, X. L. Tian, W. Chen, et al., "Analytical modeling and numerical simulation for three-roll bending forming of sheet metal," *Int. J. Adv. Manuf. Technol.*, **69**, 1639–1647 (2013).
4. M. Zhao, C. S. Wu, and P. C. Zhao, "Improvement on the accuracy of the numerical simulation of GTAW weld pool shape," *Trans. China*, **73**, No. 03, 167–170 (2006).
5. *The Welding Handbook* [in Chinese], Welding Society of Chinese Mechanical Engineering Society, Machinery Industry Press (2006), pp. 132–169.
6. B. Y. Huang, *Handbook of Materials of Nonferrous Metals* [in Chinese], Chemical Industry Press, Beijing (2009), pp. 9–126.
7. N. Ren, H. Yang, M. Zhan, et al., "Effect of weld characteristics on the formability of welded tubes in NC bending process," *Int. J. Adv. Manuf. Technol.*, **69**, 181–195 (2013).
8. Q. Y. Shi, T. L. Dickerson, and H. R. Shercliff, "Thermomechanical FE modeling of friction stir welding of Al-2024 including tool loads," in: Proc. of 4th Int. Symp. on Friction Stir Welding (May 14–16, 2003, Park City, UT, USA).
9. W. J. Qin and C. Dong, "FEM simulation of quenching process and investigation of residual stresses of crankshafts," *Key Eng. Mat.*, **626**, 149–153 (2014).
10. H. Kubota, A. Tomizawa, K. Yamamoto, and N. Okada, "Development of finite element analysis method for three-dimensional hot bending and direct quench (3DQ) process," *AIP Conf. Proc.*, **1532**, 568–572 (2013).
11. H. Y. Fang, *Welding Structure* [in Chinese], Mechanical Industry Press (2011), pp. 64–71.
12. N. C. Lü, "Laws on welding angular distortion on cylindrical plate of LF6Y2 aluminum alloy welding angular deformation rules," *Mater. Sci. Technol.* [in Chinese], **12**, No. 3, 317–319 (2004).